Flexible, Foldable, Actively Multiplexed, High-Density Electrode Array for Mapping Brain Activity *in vivo*

Jonathan Viventi[1,2⊥], Dae-Hyeong Kim[3⊥], Leif Vigeland[4], Eric S. Frechette[5], Justin A. Blanco[6], Yun-Soung Kim[7], Andrew E. Avrin[8], Vineet R. Tiruvadi[9], Suk-Won Hwang[7], Ann C. Vanleer[9], Drausin F. Wulsin[9], Kathryn Davis[5], Casey E. Gelber[9], Larry Palmer[4], Jan Van der Spiegel[8], Jian Wu[10], Jianliang Xiao[11], Yonggang Huang[12], Diego Contreras[4], John A. Rogers[7], Brian Litt[5,9*]

[1]*Department of Electrical and Computer Engineering, Polytechnic Institute of New York University, Brooklyn, NY 11201 USA*

[2]*Center for Neural Science, New York University, New York, NY 10003 USA*

[3]*School of Chemical and Biological Engineering, Seoul National University, Seoul 151-744 Korea*

[4]*Department of Neuroscience, University of Pennsylvania School of Medicine, 215 Stemmler Hall, Philadelphia, PA 19104 USA*

[5]*Department of Neurology, Hospital of the University of Pennsylvania, 3 West Gates, 3400 Spruce Street, Philadelphia, PA 19104 USA*

[6]*Department of Electrical and Computer Engineering, United States Naval Academy, Annapolis, MD 21402 USA*

[7]*Department of Materials Science and Engineering, Beckman Institute for Advanced Science and Technology and Frederick Seitz Materials Research Laboratory, University of Illinois at Urbana-Champaign, Urbana, Illinois 61801 USA*

[8]*Department of Electrical and Systems Engineering, University of Pennsylvania, Philadelphia, PA 19104 USA*

[9]*Department of Bioengineering, University of Pennsylvania, Philadelphia, PA 19104 USA*

[10]*AML, Department of Engineering Mechanics, Tsinghua Univeristy, Beijing 100084, China*

Nature Neuroscience: doi:10.1038/nn.2973

[11]*Department of Mechanical Engineering, University of Colorado Boulder, Boulder, CO 80309 USA*

[12]*Departments of Civil and Environmental Engineering and Mechanical Engineering, Northwestern University, Evanston, IL 60208*

⊥ *J. Viventi and D.-H. Kim contributed equally.*

*To whom correspondence should be addressed. *E-mail:* *littb@mail.med.upenn.edu*; *jrogers@uiuc.edu*

Supplementary Movie 1. Movie of a short electrographic seizure showing numerous complicated spatial patterns, including clockwise and counterclockwise spiral waves. The voltage for all 360 channels is plotted as a color map in the top of the frame, while the average of all 360 electrodes is plotted at the bottom of the frame with a vertical bar indicating the position in time for reference. The movie is presented ~18× slower than real-time. (MPEG; 29.3 MB).

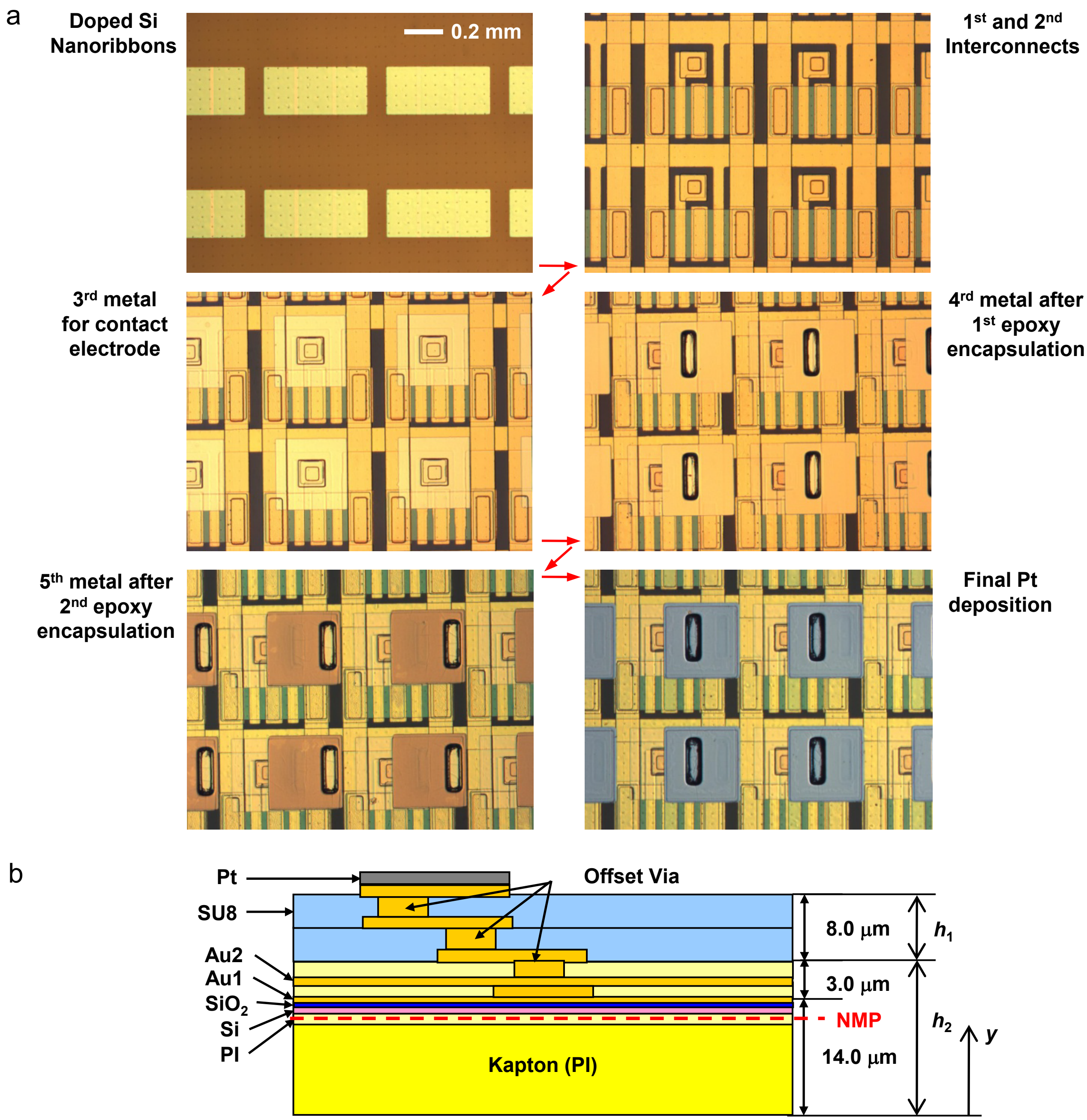

Supplementary Figure 1. Schematic of fabrication steps **a,** Microscope images of each fabrication step. **b,** schematic cross-sectional information, red dotted line shows the location of neutral mechanical plane (NMP).

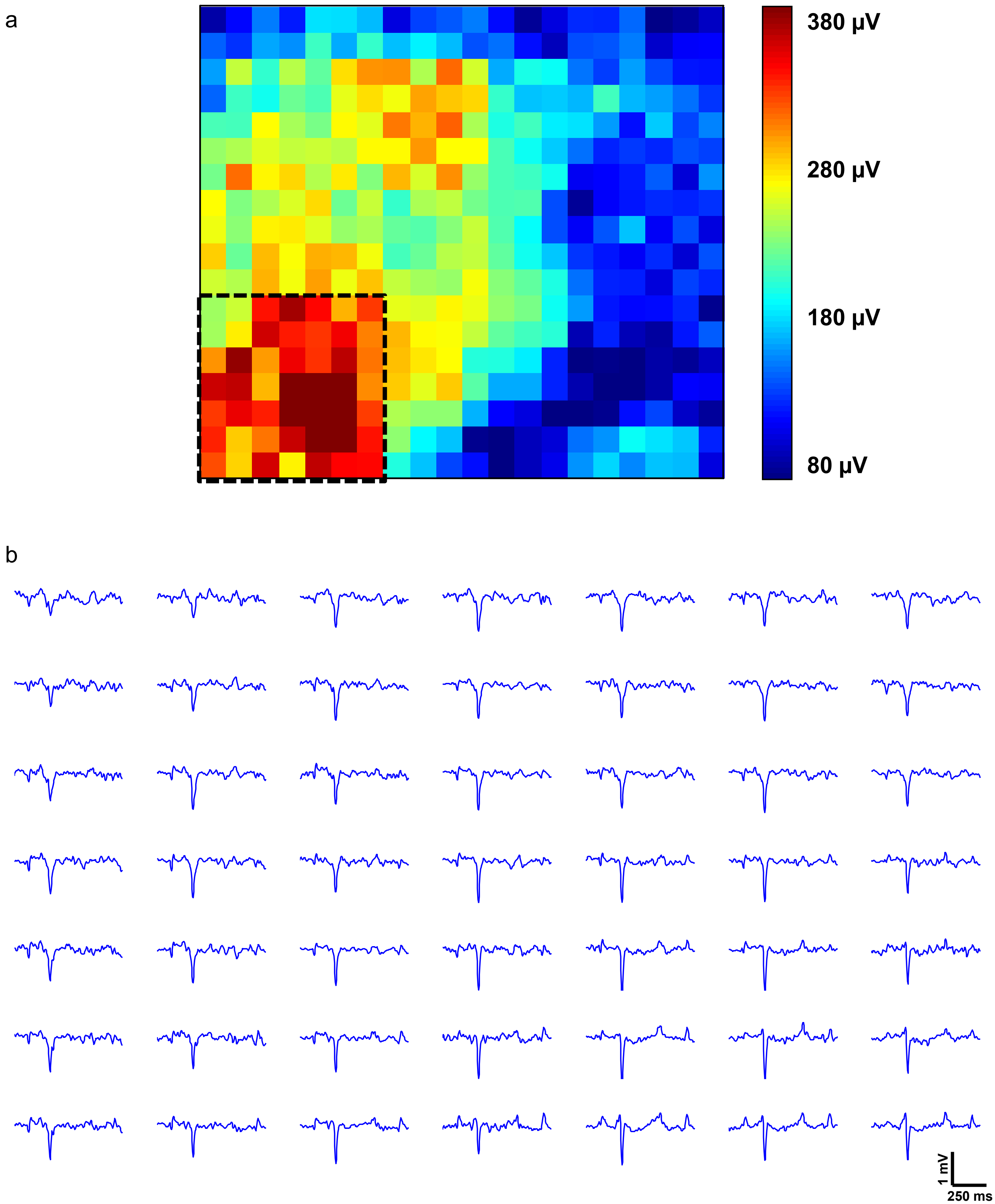

Supplementary Figure 2. A single-trial visual evoked potential from a full-field drifting grating. **a,** Spatial distribution of the visual evoked response, as determined by the root-mean-square (RMS) value of the zero-meaned signal within the 40 ms to 160 ms window after the stimulus. Data are anatomically orientated as shown in the inset of **Figure 3b**. **b,** Individual visual evoked responses shown for the 49 electrodes located in the bottom, left-hand corner of the electrode array, as highlighted by the dashed box above.

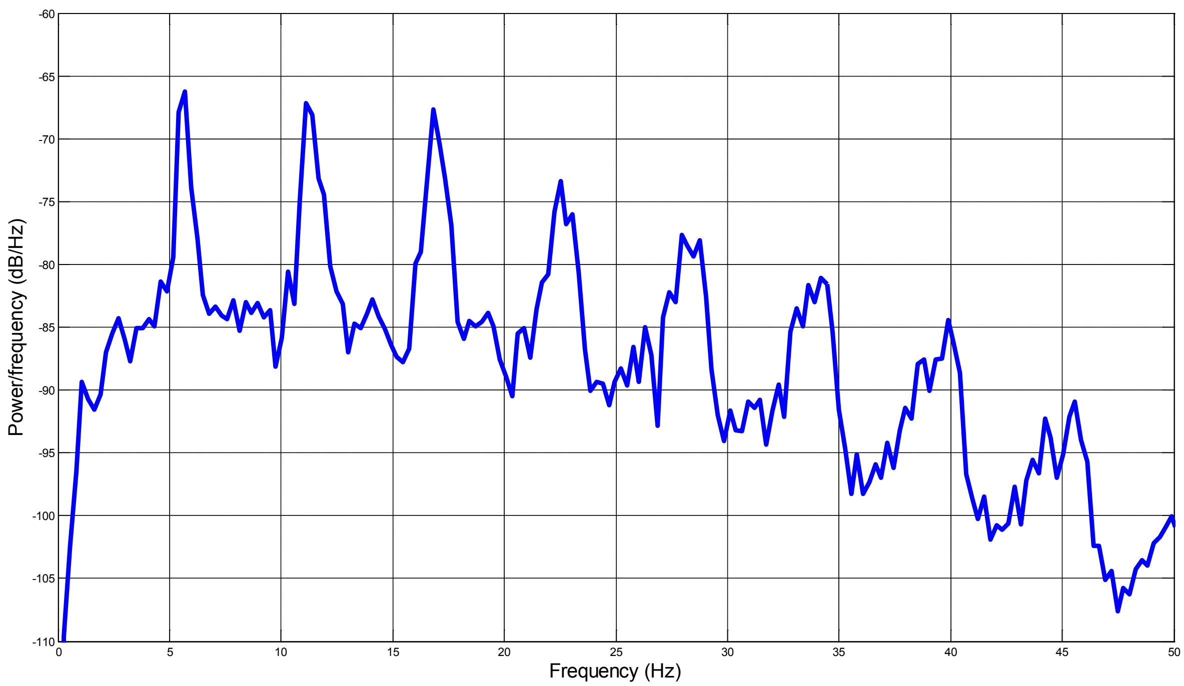

Supplementary Figure 3. Analysis of the frequency content of a sustained, counter-clockwise spiral during a short seizure. The primary frequency component was 6 Hz. The power spectral density was calculated using 'pwelch' with a window size of 1024 on each channel of the electrode array individually. The resulting power spectra were averaged to produce a single overall power spectral density.

a

Cluster 1

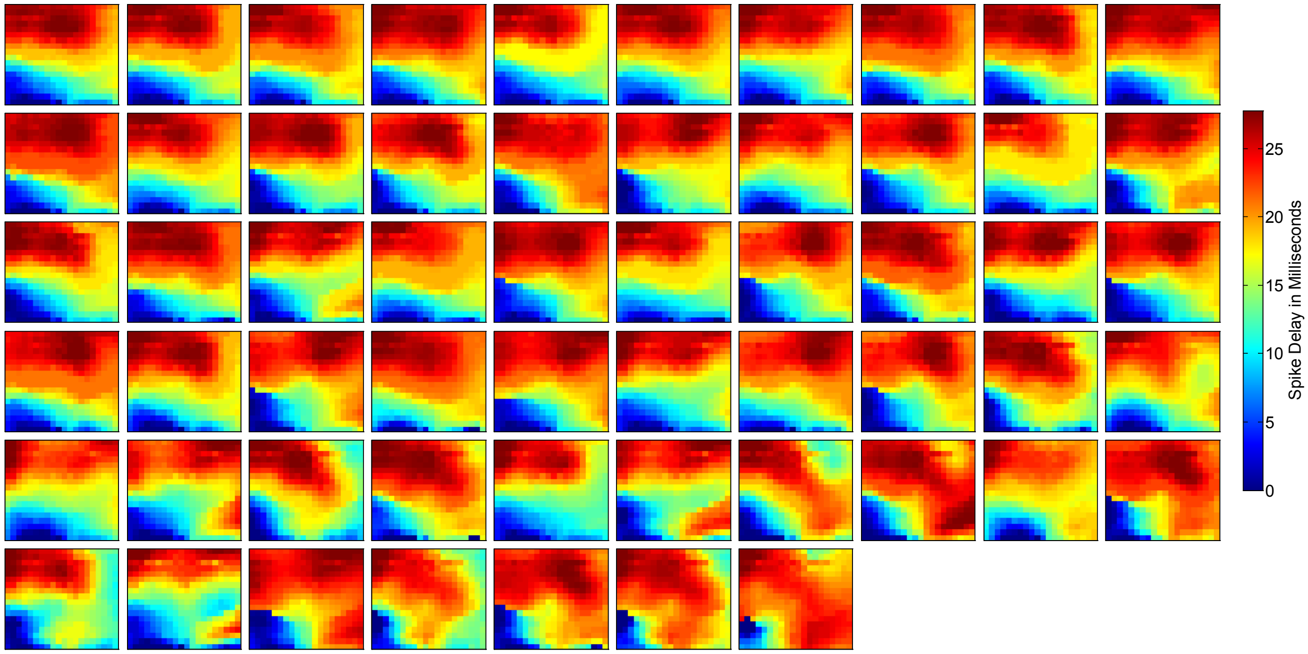

b

Cluster 2

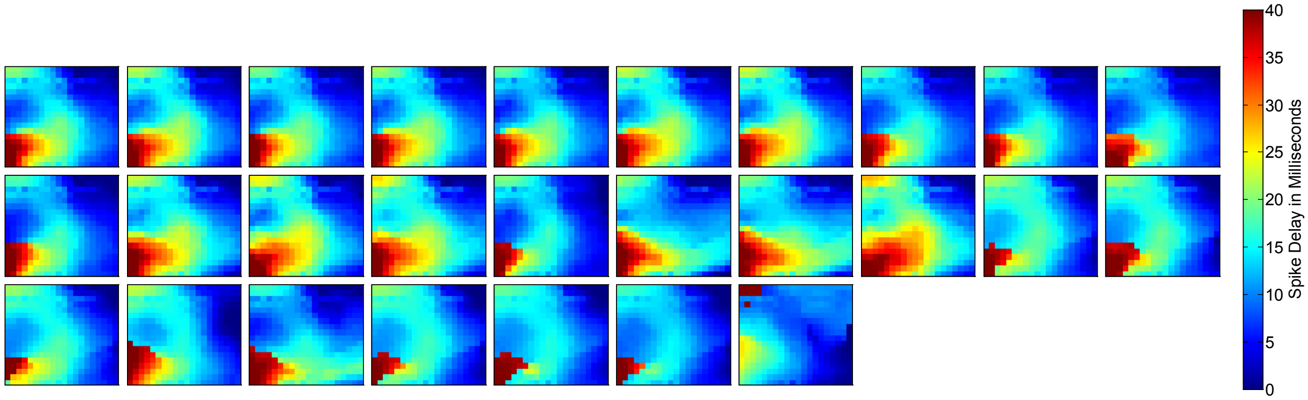

Supplementary Figure 4. Delay maps for all of the spikes in each cluster indicated a strong similarity within clusters. The spikes in clusters 2, 4, 12, 14, and 19 appeared to occur almost exclusively during seizures, while spikes in the other clusters appeared to occur uniformly throughout the record.

a

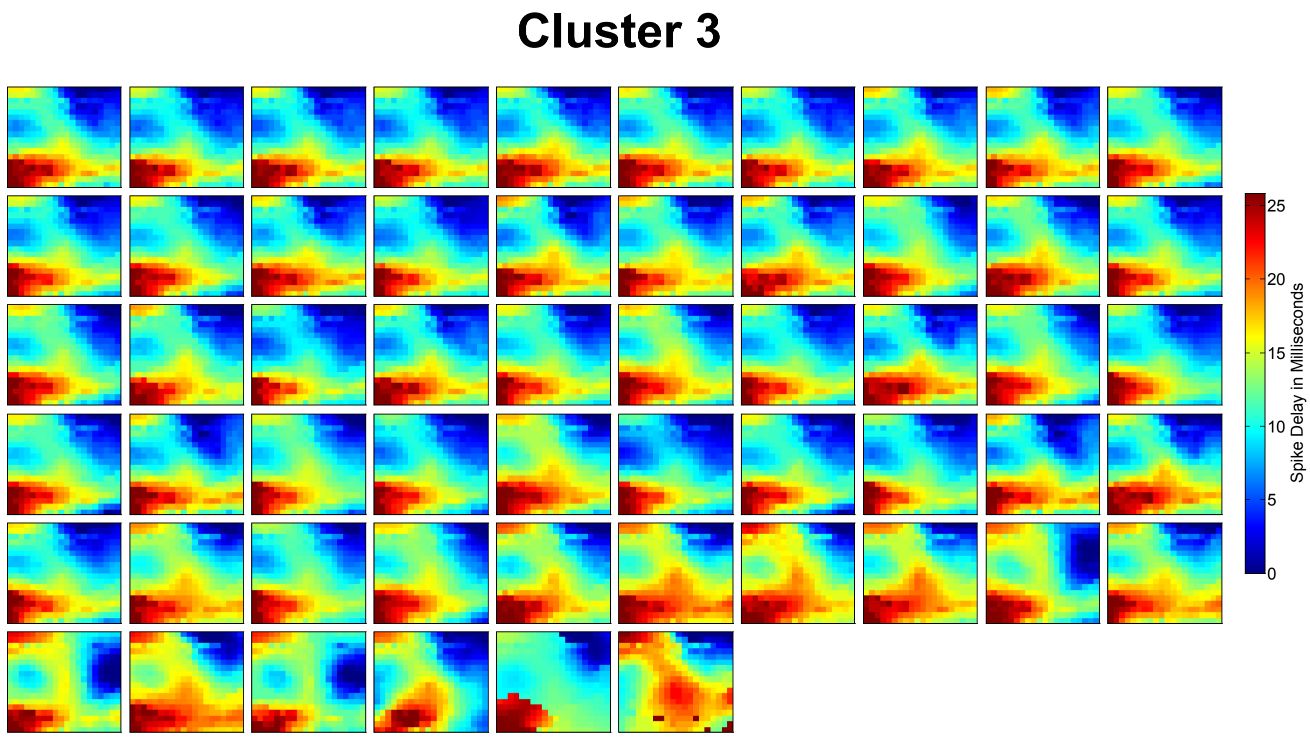

b

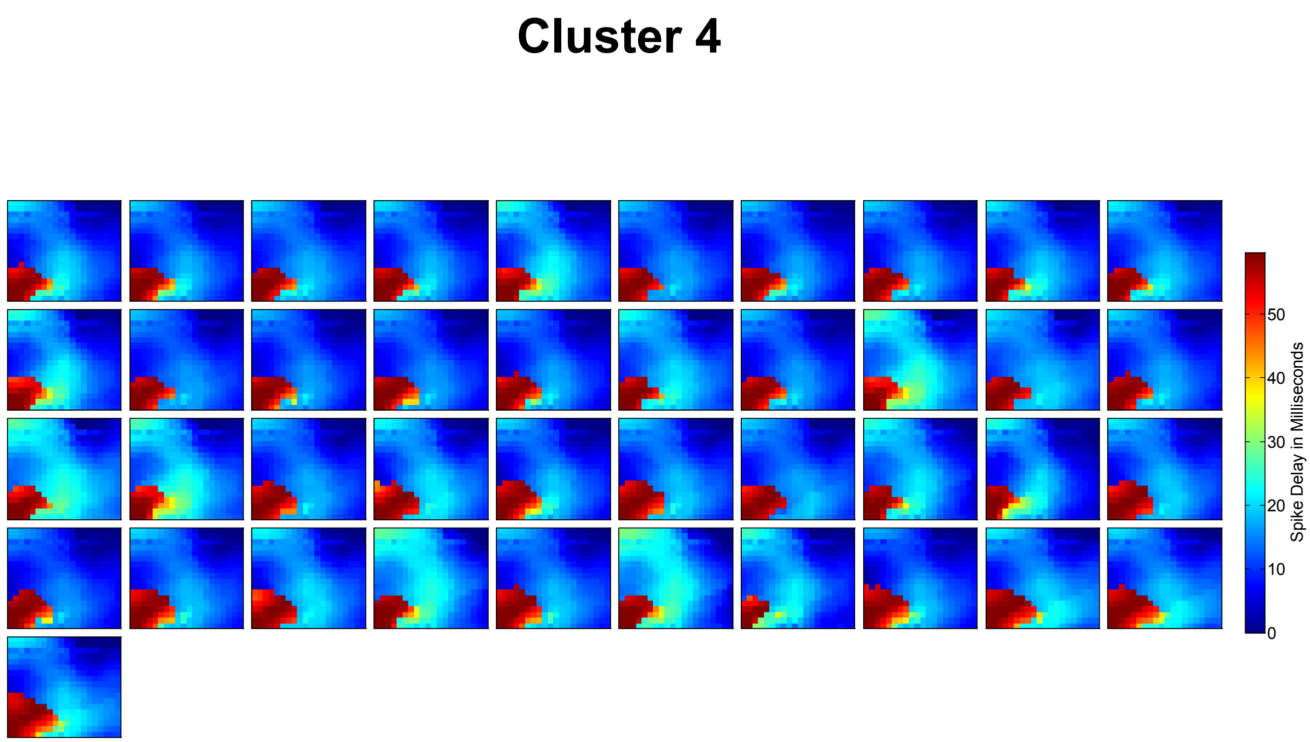

Supplementary Figure 5. Delay maps for all of the spikes in each cluster indicated a strong similarity within clusters. The spikes in clusters 2, 4, 12, 14, and 19 appeared to occur almost exclusively during seizures, while spikes in the other clusters appeared to occur uniformly throughout the record.

a

Cluster 5

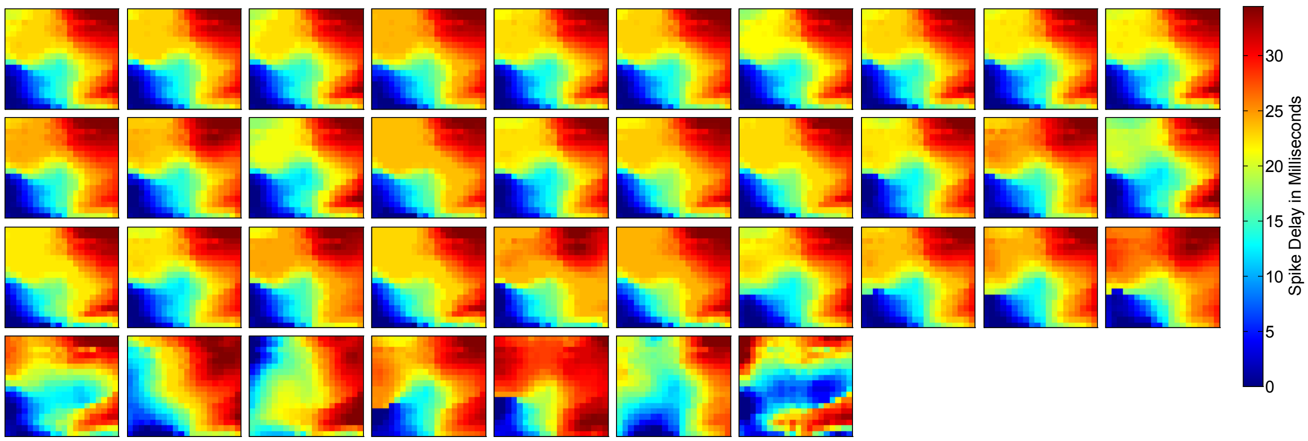

b

Cluster 6

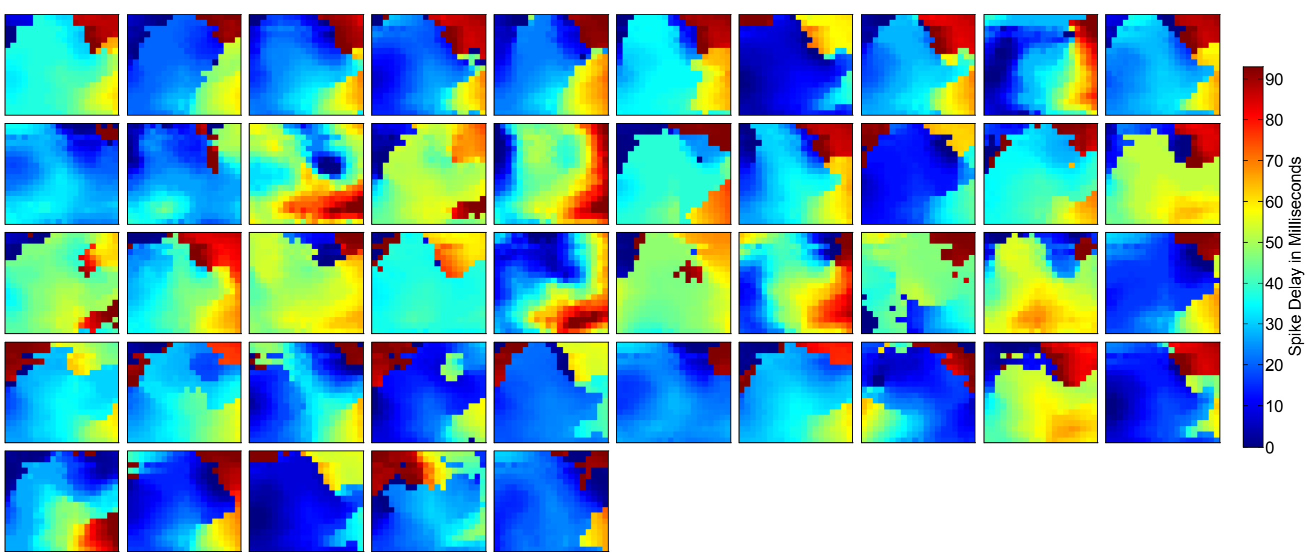

Supplementary Figure 6. Delay maps for all of the spikes in each cluster indicated a strong similarity within clusters. The spikes in clusters 2, 4, 12, 14, and 19 appeared to occur almost exclusively during seizures, while spikes in the other clusters appeared to occur uniformly throughout the record.

Nature Neuroscience: doi:10.1038/nn.2973

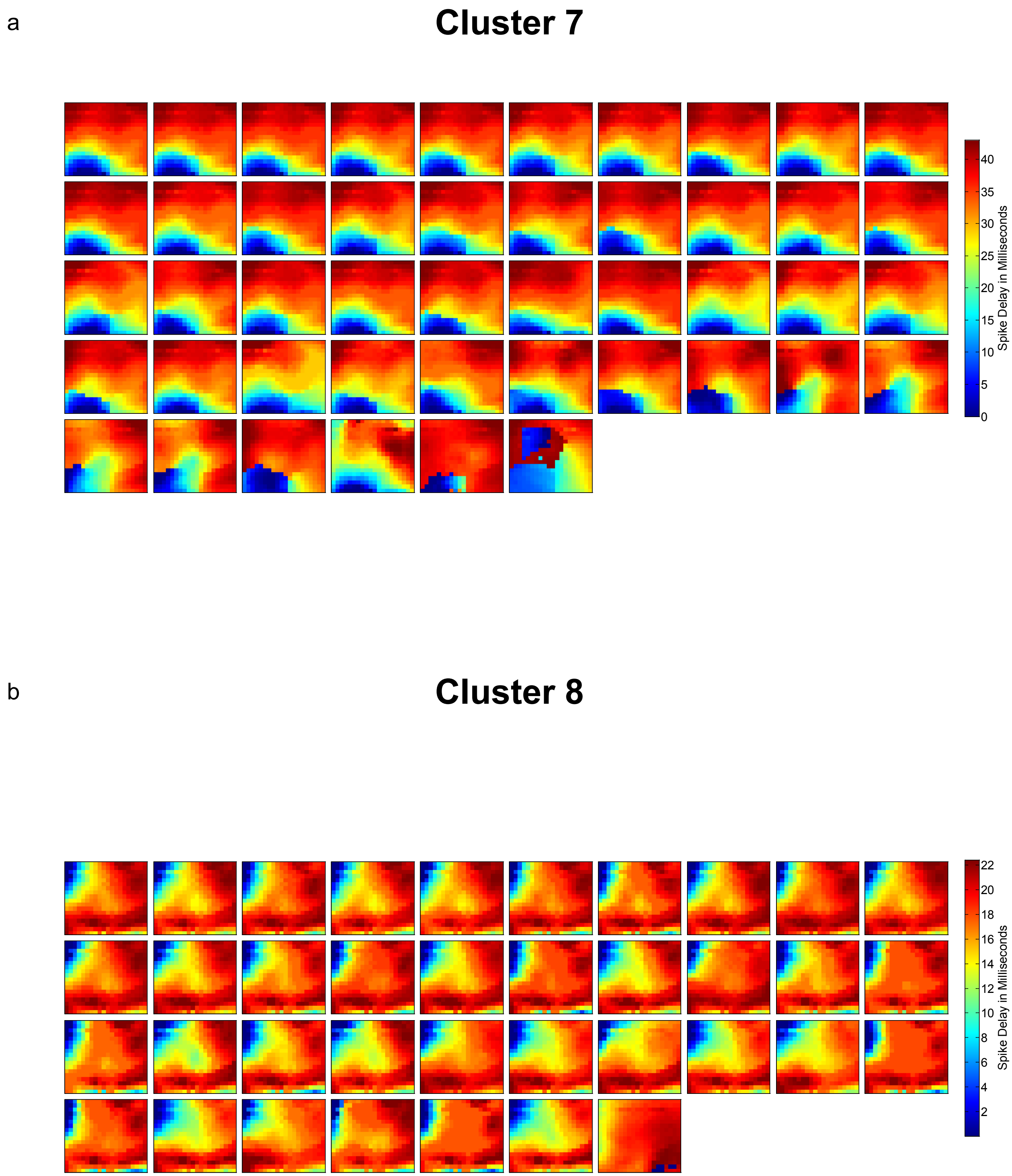

Supplementary Figure 7. Delay maps for all of the spikes in each cluster indicated a strong similarity within clusters. The spikes in clusters 2, 4, 12, 14, and 19 appeared to occur almost exclusively during seizures, while spikes in the other clusters appeared to occur uniformly throughout the record.

a

Cluster 9

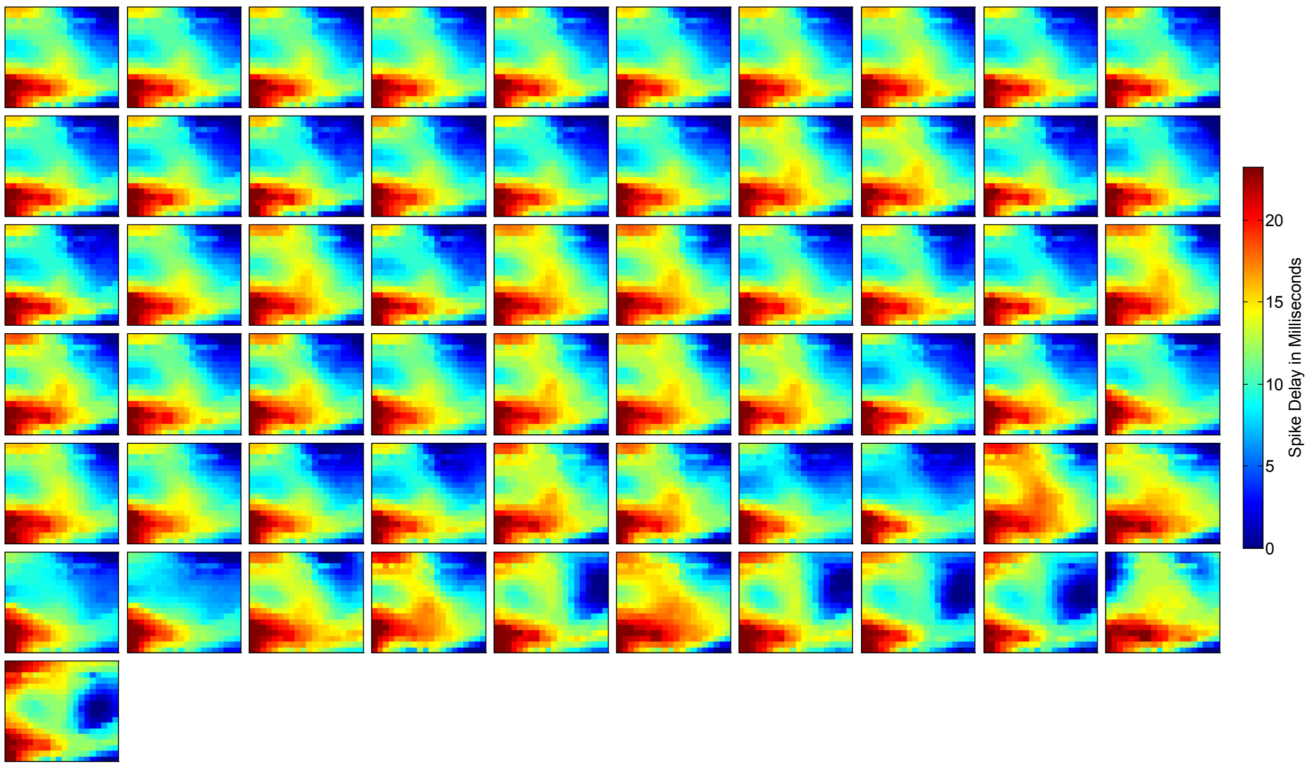

b

Cluster 10

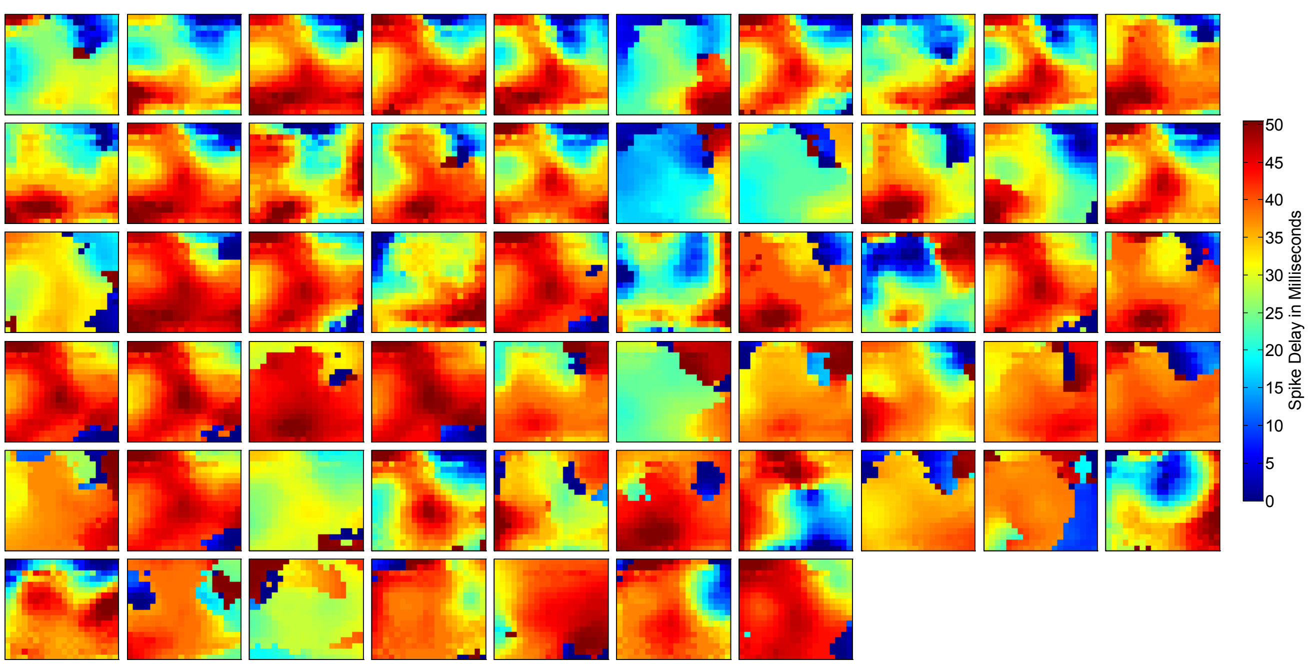

Supplementary Figure 8. Delay maps for all of the spikes in each cluster indicated a strong similarity within clusters. The spikes in clusters 2, 4, 12, 14, and 19 appeared to occur almost exclusively during seizures, while spikes in the other clusters appeared to occur uniformly throughout the record.

Nature Neuroscience: doi:10.1038/nn.2973

a

Cluster 11

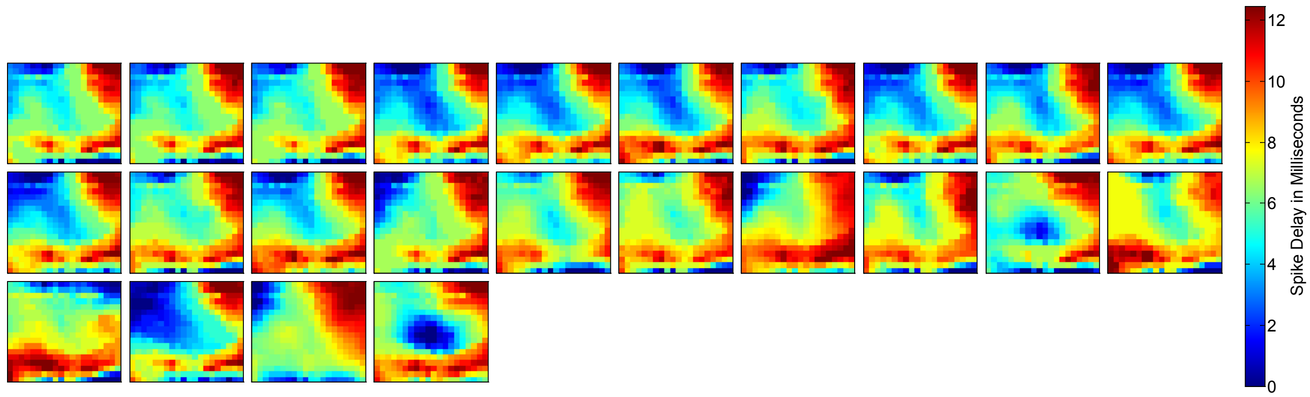

b

Cluster 12

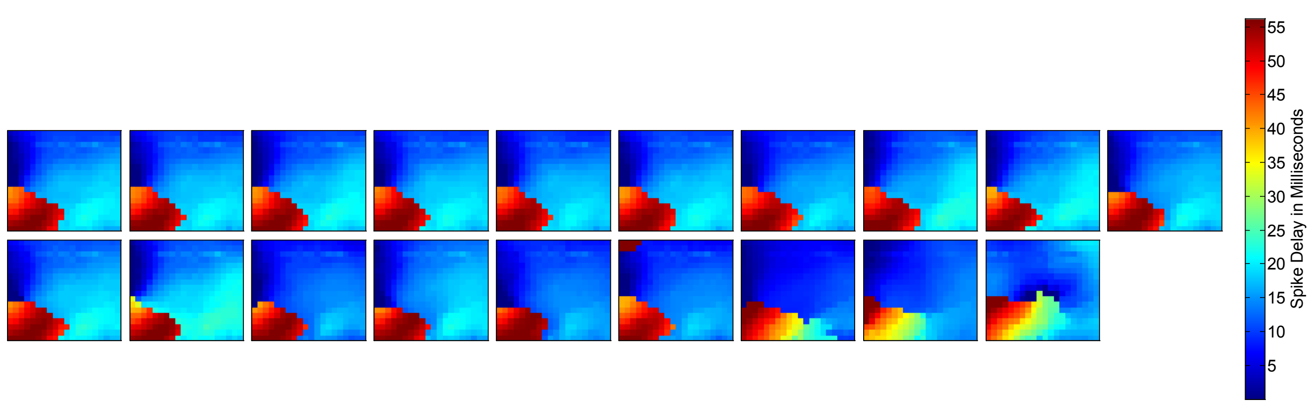

Supplementary Figure 9. Delay maps for all of the spikes in each cluster indicated a strong similarity within clusters. The spikes in clusters 2, 4, 12, 14, and 19 appeared to occur almost exclusively during seizures, while spikes in the other clusters appeared to occur uniformly throughout the record.

a

Cluster 13

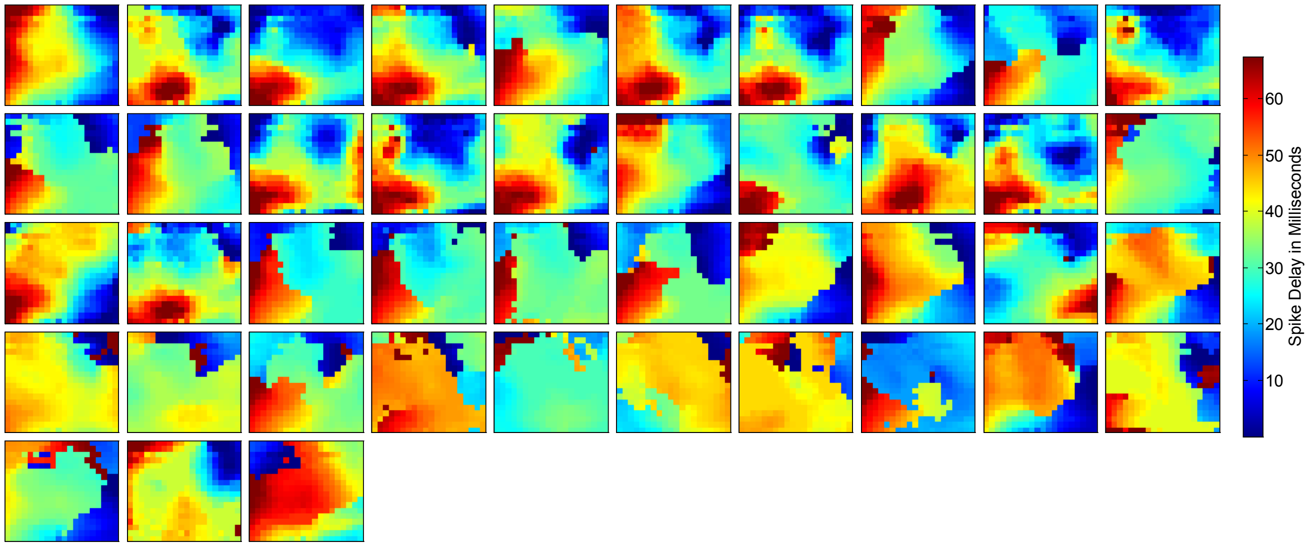

b

Cluster 14

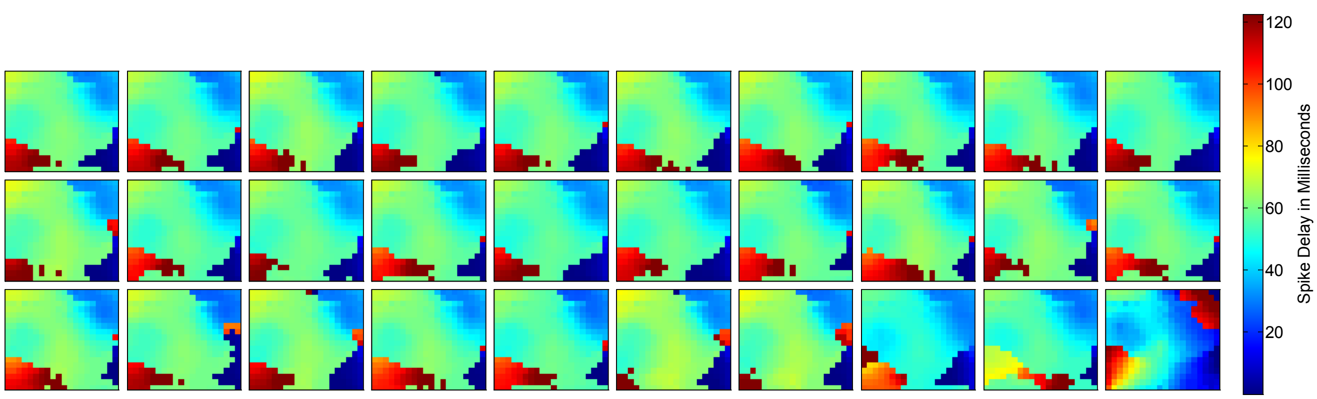

Supplementary Figure 10. Delay maps for all of the spikes in each cluster indicated a strong similarity within clusters. The spikes in clusters 2, 4, 12, 14, and 19 appeared to occur almost exclusively during seizures, while spikes in the other clusters appeared to occur uniformly throughout the record.

a

Cluster 15

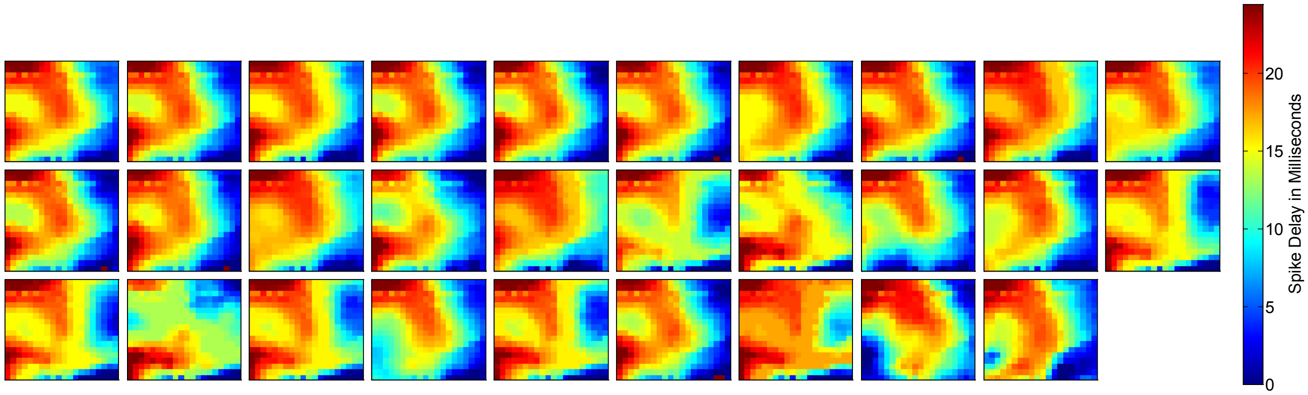

b

Cluster 16

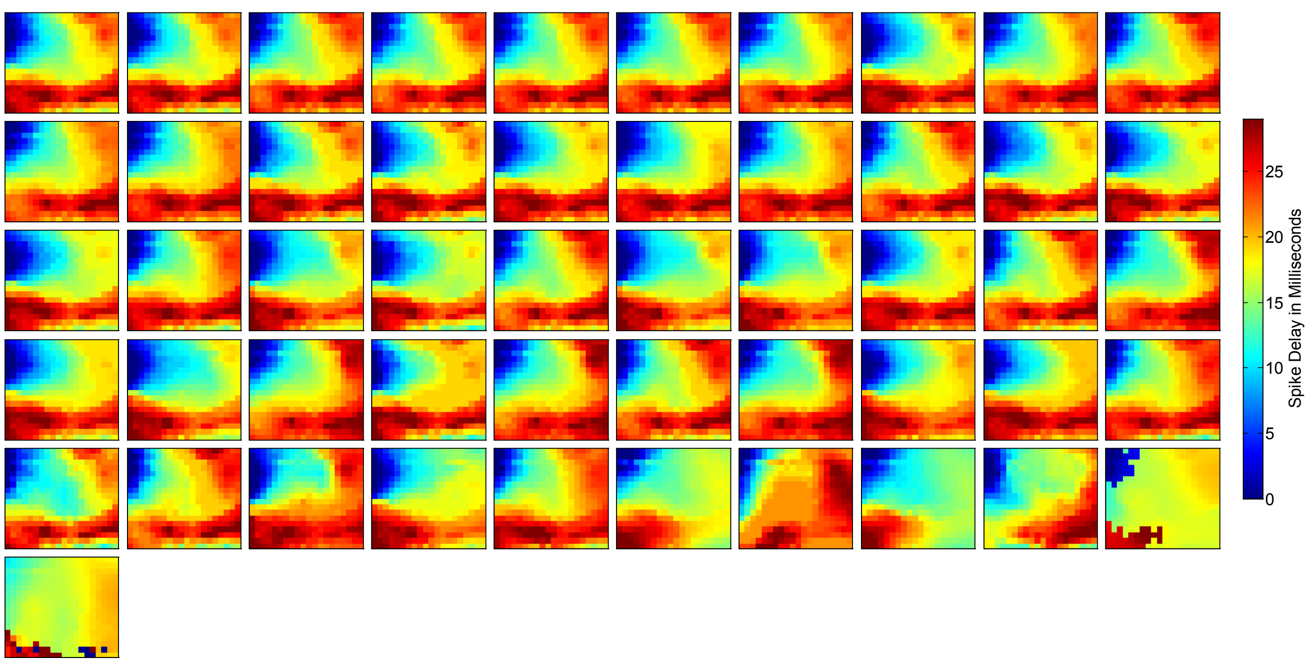

Supplementary Figure 11. Delay maps for all of the spikes in each cluster indicated a strong similarity within clusters. The spikes in clusters 2, 4, 12, 14, and 19 appeared to occur almost exclusively during seizures, while spikes in the other clusters appeared to occur uniformly throughout the record.

a

Cluster 17

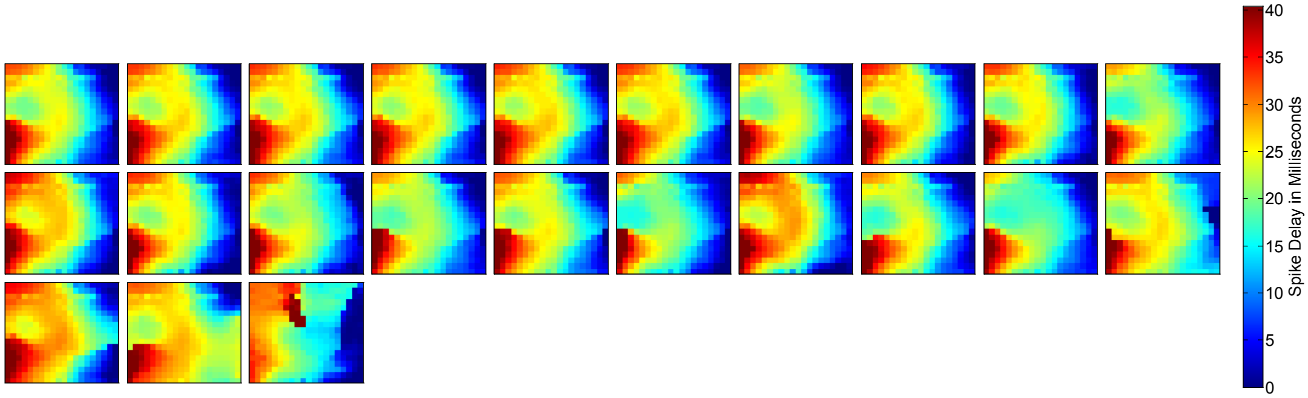

b

Cluster 18

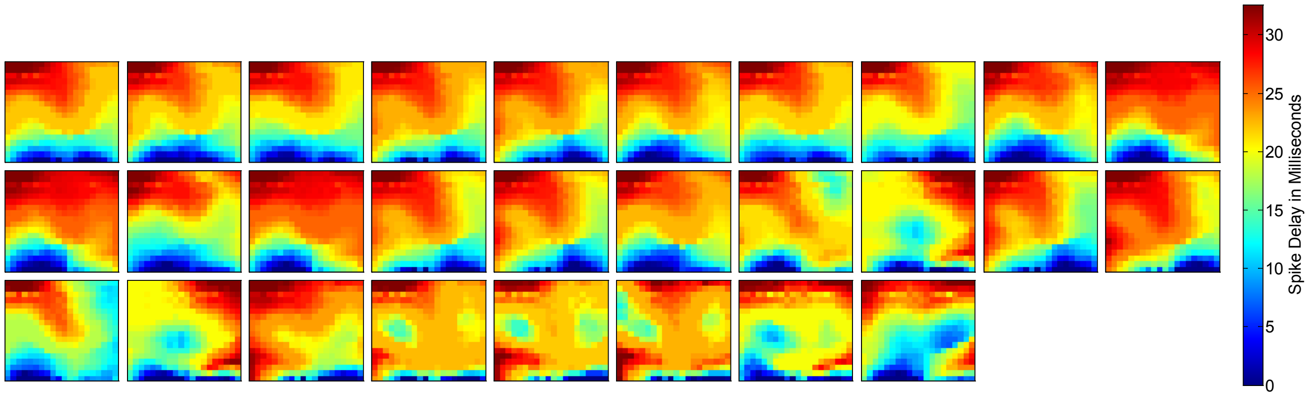

Supplementary Figure 12. Delay maps for all of the spikes in each cluster indicated a strong similarity within clusters. The spikes in clusters 2, 4, 12, 14, and 19 appeared to occur almost exclusively during seizures, while spikes in the other clusters appeared to occur uniformly throughout the record.

a

Cluster 19

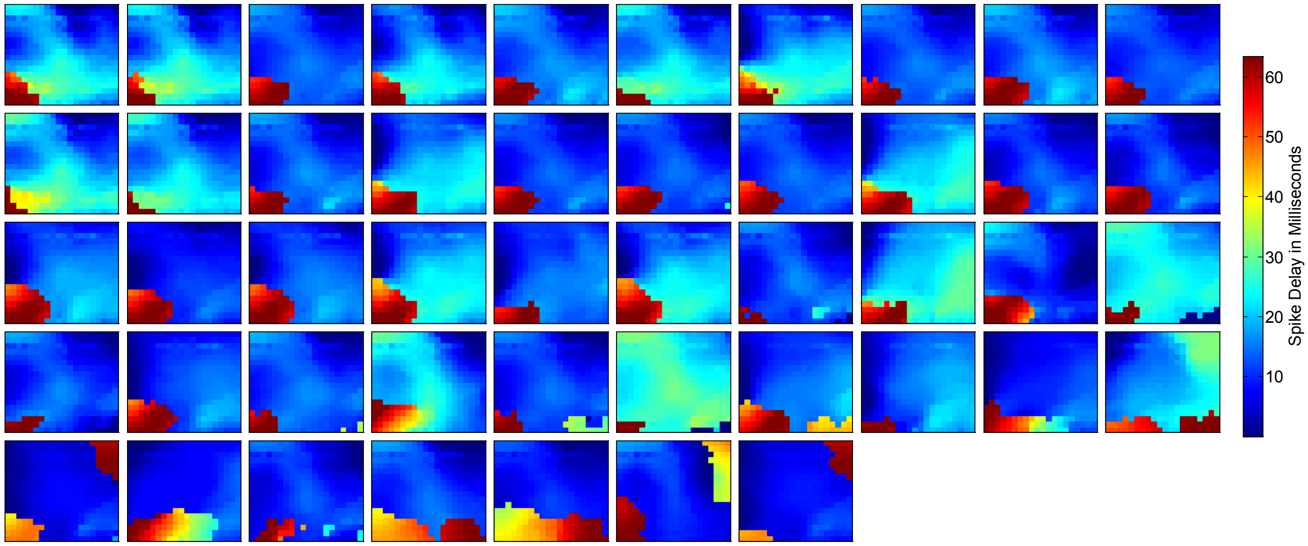

b

Cluster 20

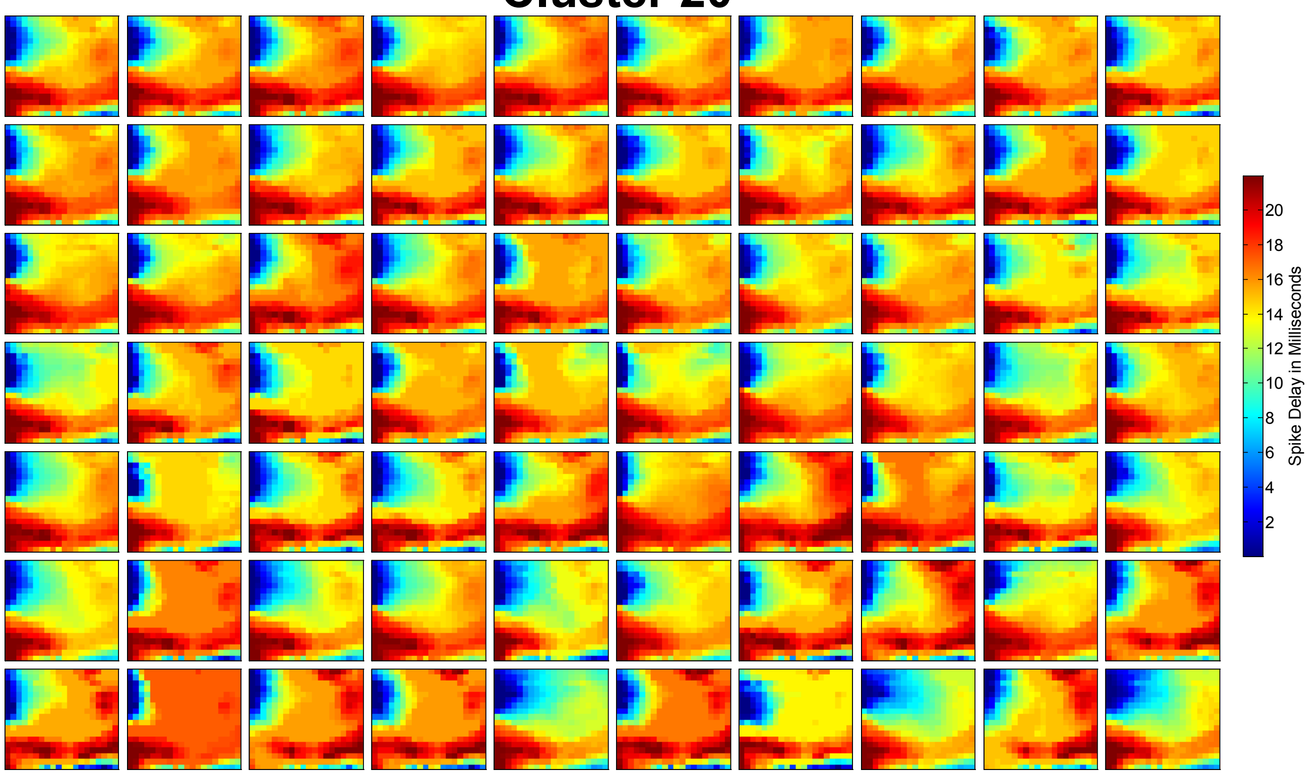

Supplementary Figure 13. Delay maps for all of the spikes in each cluster indicated a strong similarity within clusters. The spikes in clusters 2, 4, 12, 14, and 19 appeared to occur almost exclusively during seizures, while spikes in the other clusters appeared to occur uniformly throughout the record.

a

Cluster 21

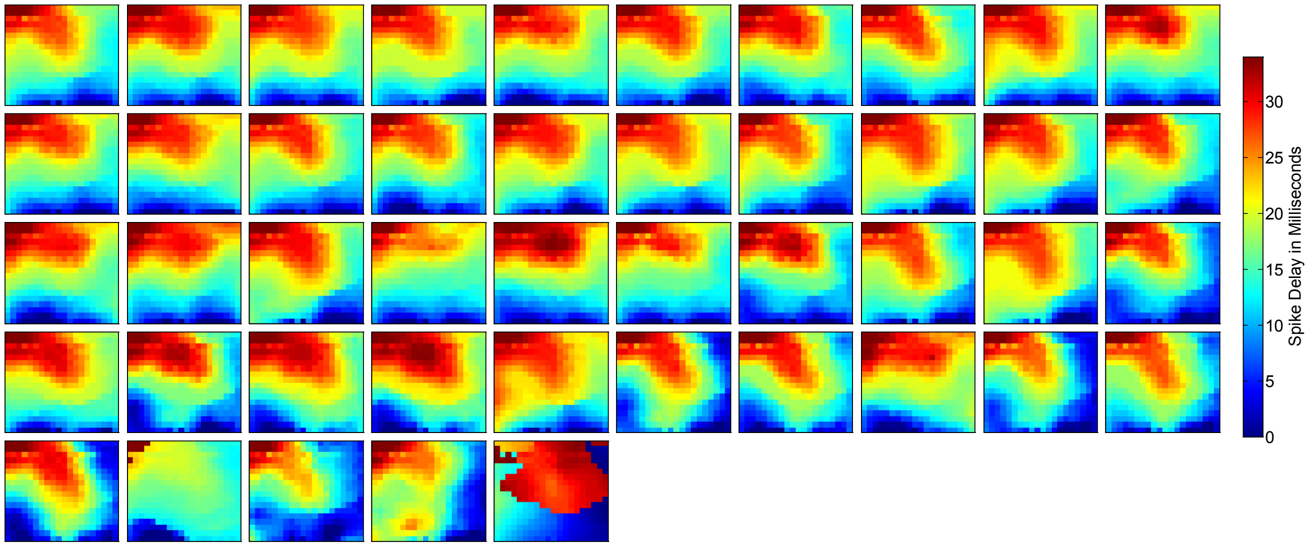

Supplementary Figure 14. Delay maps for all of the spikes in each cluster indicated a strong similarity within clusters. The spikes in clusters 2, 4, 12, 14, and 19 appeared to occur almost exclusively during seizures, while spikes in the other clusters appeared to occur uniformly throughout the record.

Nature Neuroscience: doi:10.1038/nn.2973

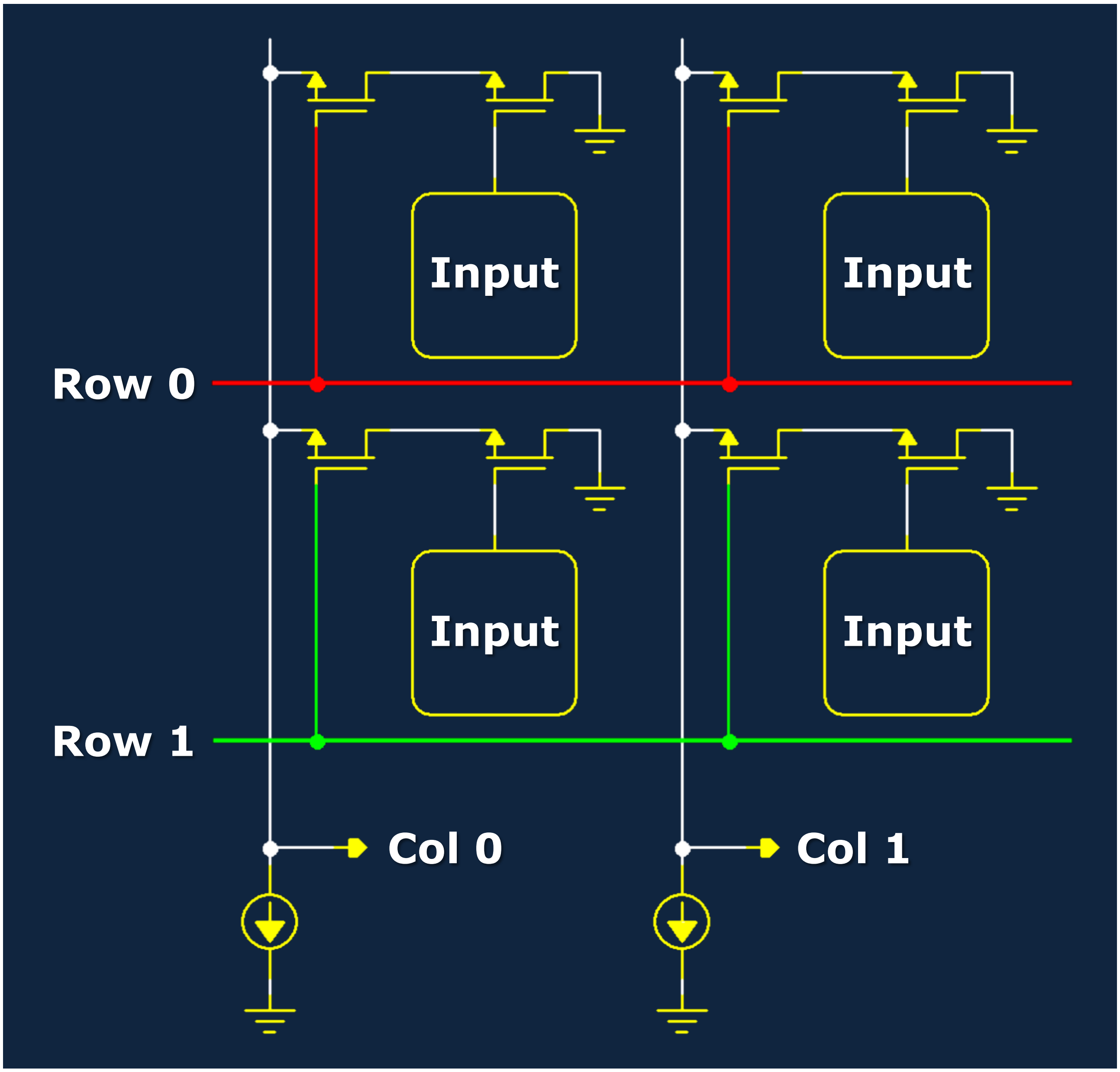

Supplementary Figure 15. Circuit diagram of four unit cells, showing multiplexing connections.

a

b

c

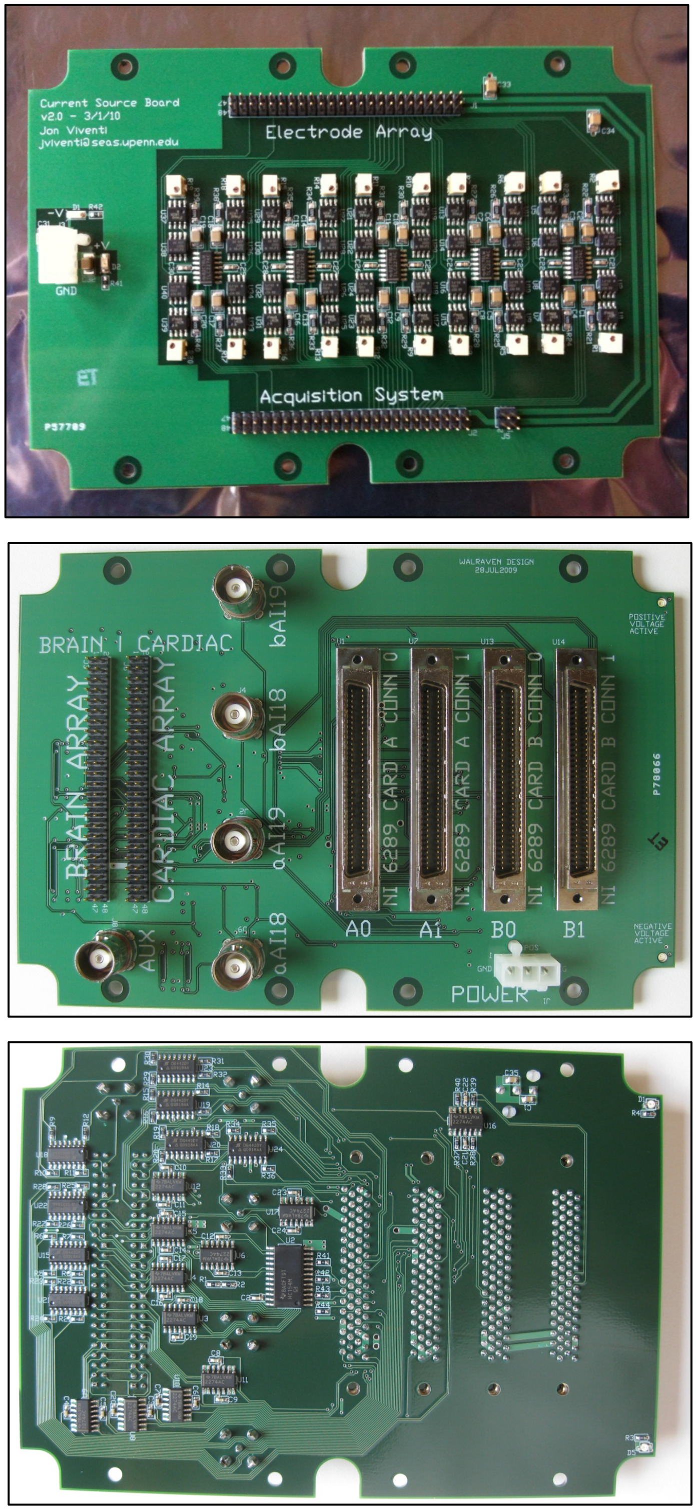

Supplementary Figure 16. Photographs of data acquisition system components. **a,** Photograph of custom circuit board that implements the off array constant current sinks, buffering and high-pass filtering. **b,** Photograph of custom data acquisition interface circuit board that generates row select signals and provides another stage of buffering (top) and **c,** (bottom).

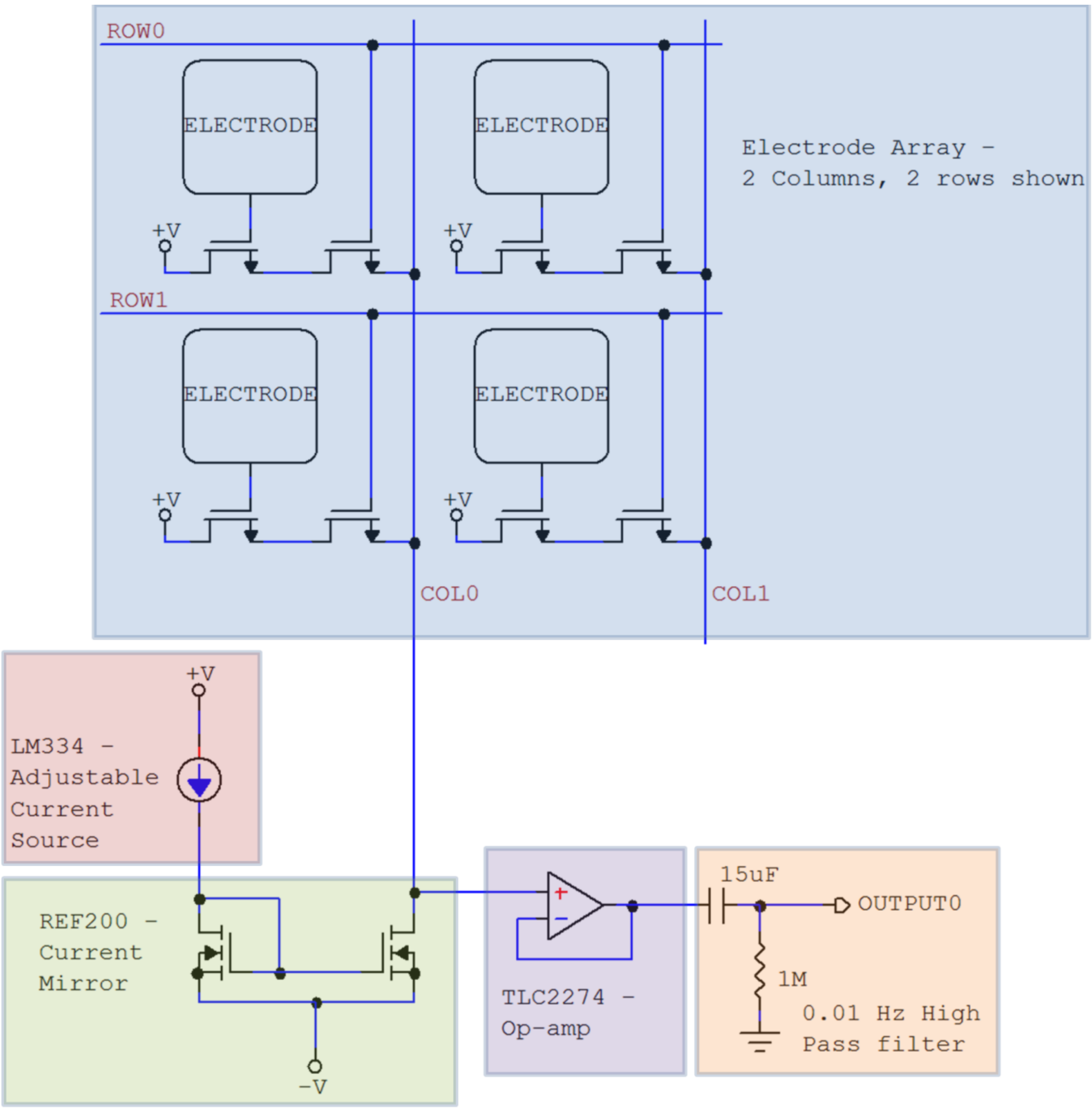

Supplementary Figure 17. Block diagram of constant current sink implementation. This circuit is repeated 20 times, one for each column of the electrode array.

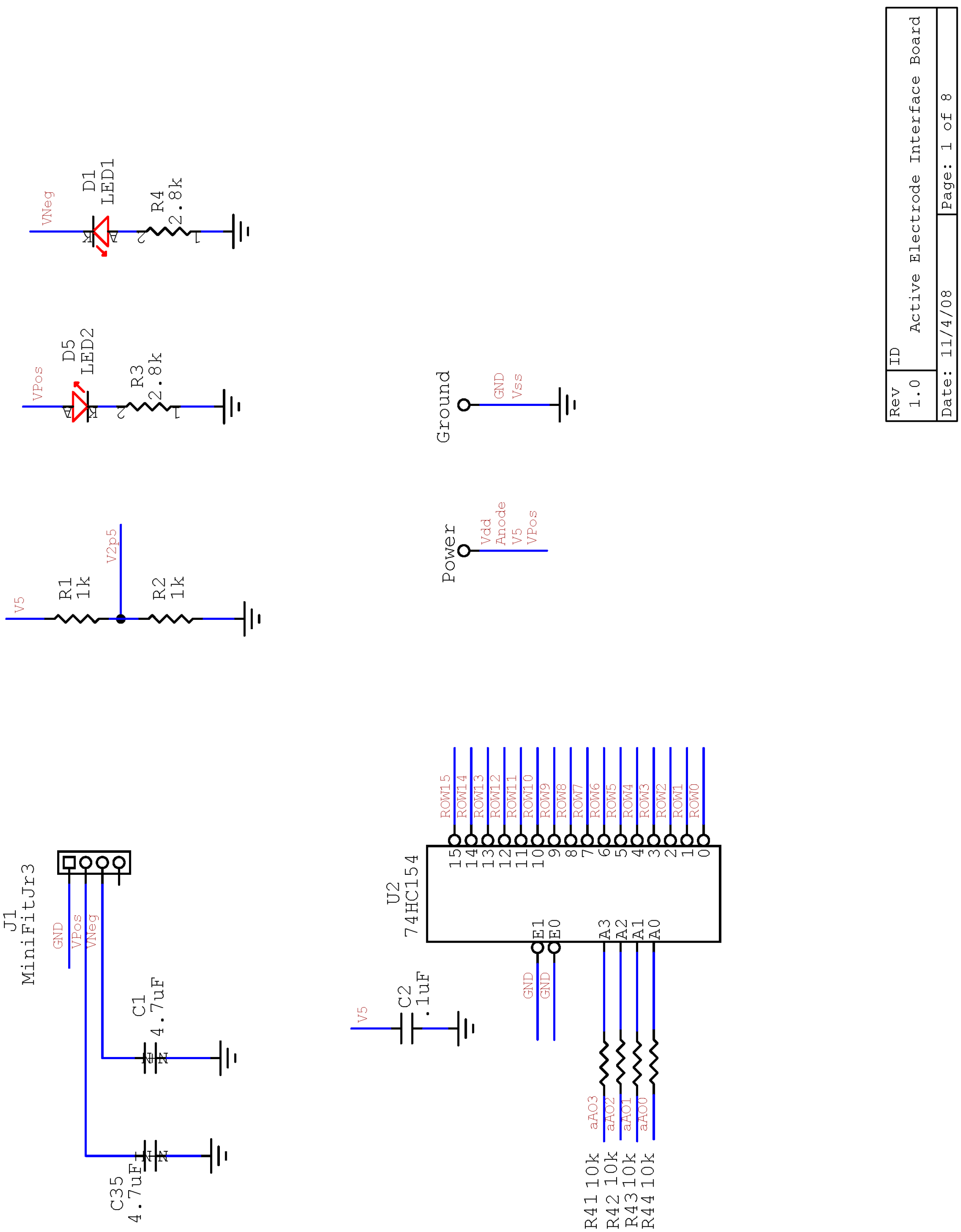

Supplementary Figure 18. Complete schematics of the custom data acquisition interface circuit board.

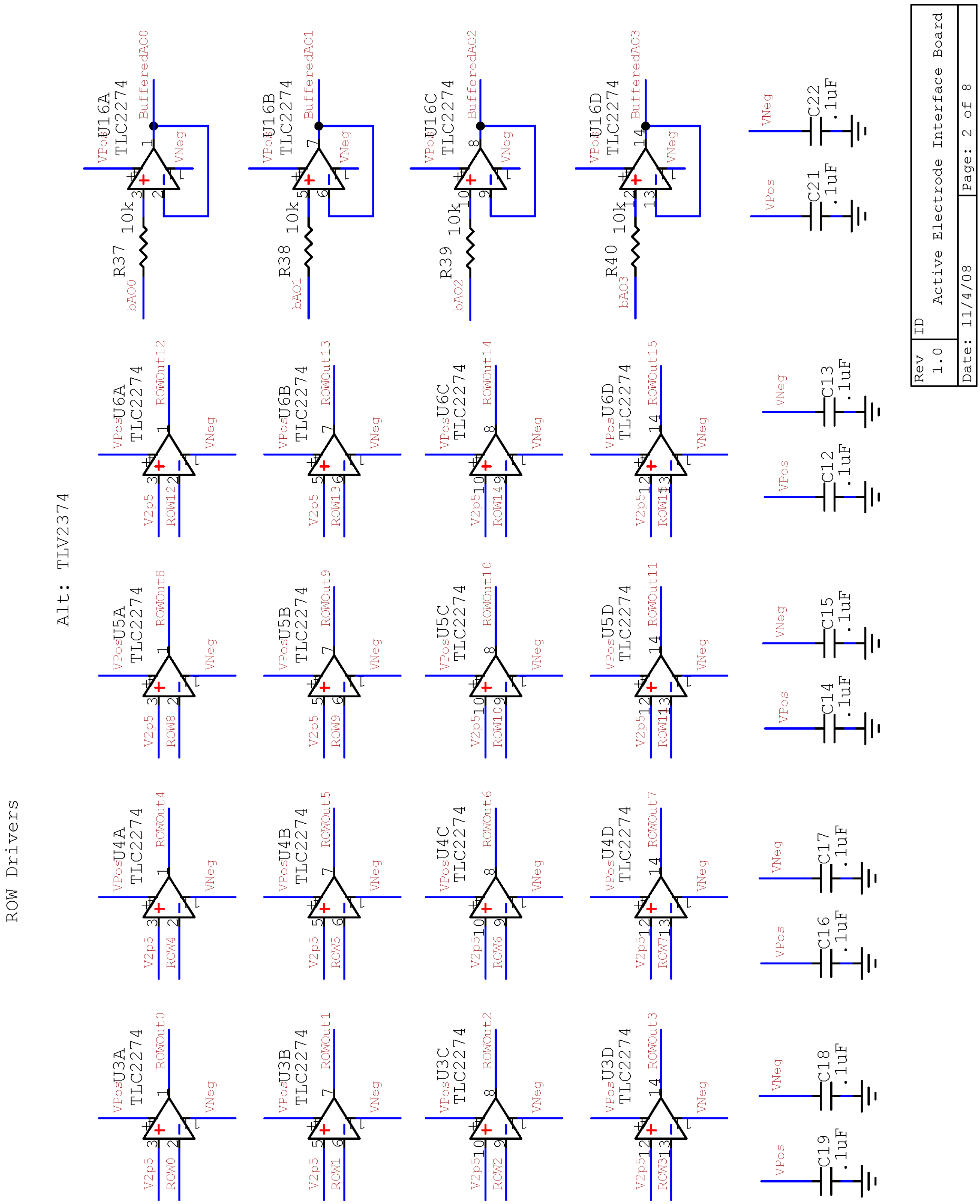

Supplementary Figure 19. Complete schematics of the custom data acquisition interface circuit board.

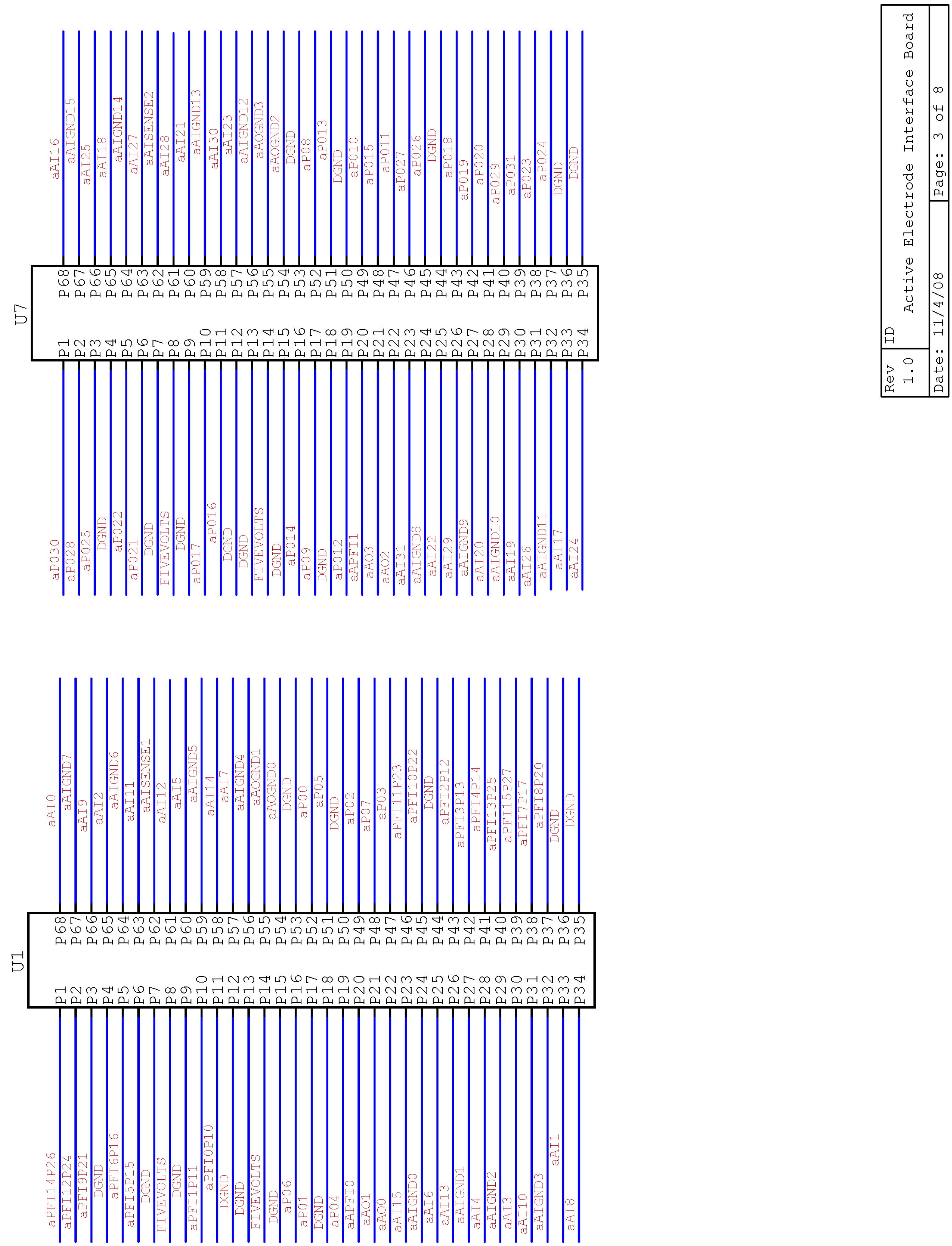

Supplementary Figure 20. Complete schematics of the custom data acquisition interface circuit board.

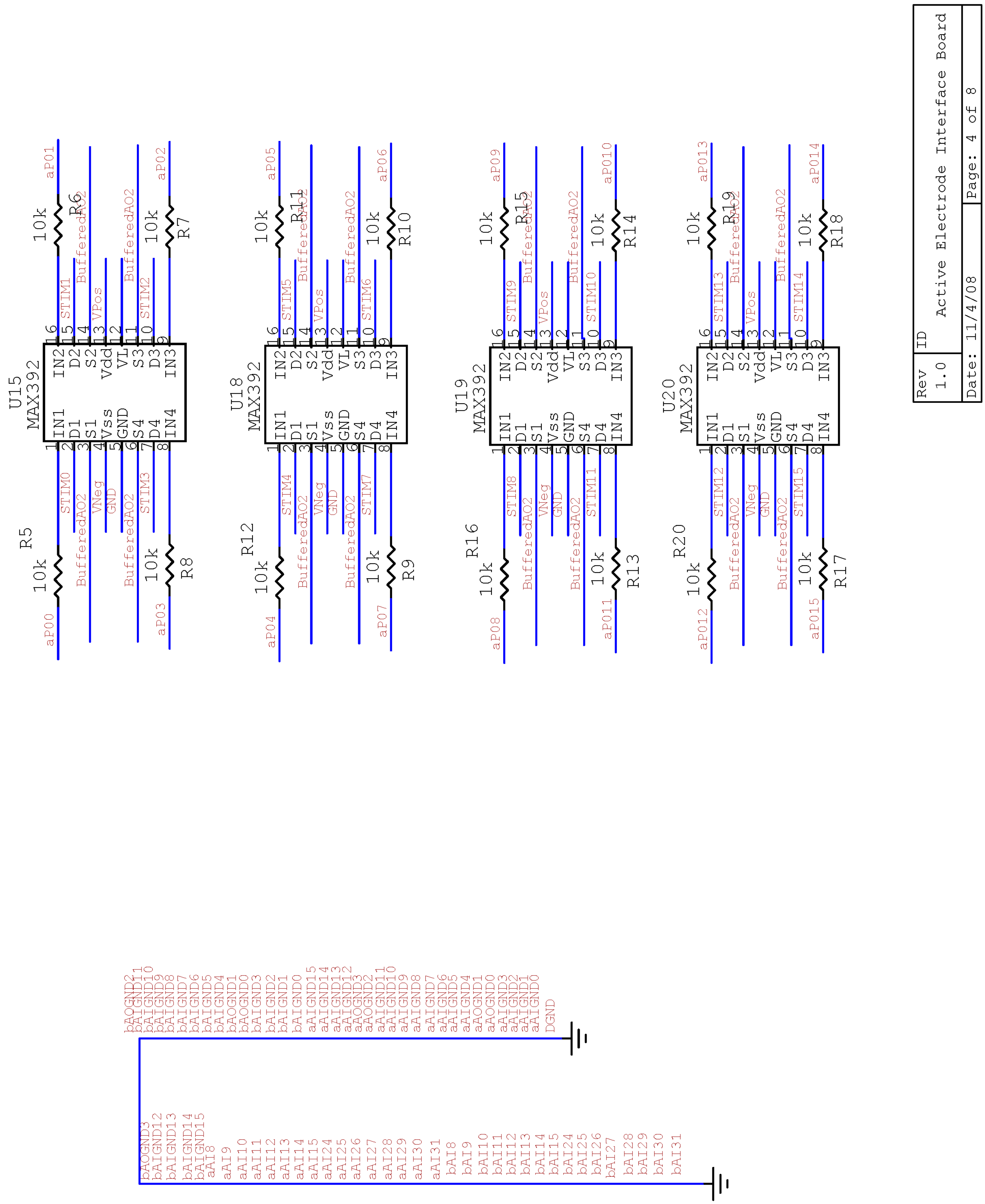

Supplementary Figure 21. Complete schematics of the custom data acquisition interface circuit board.

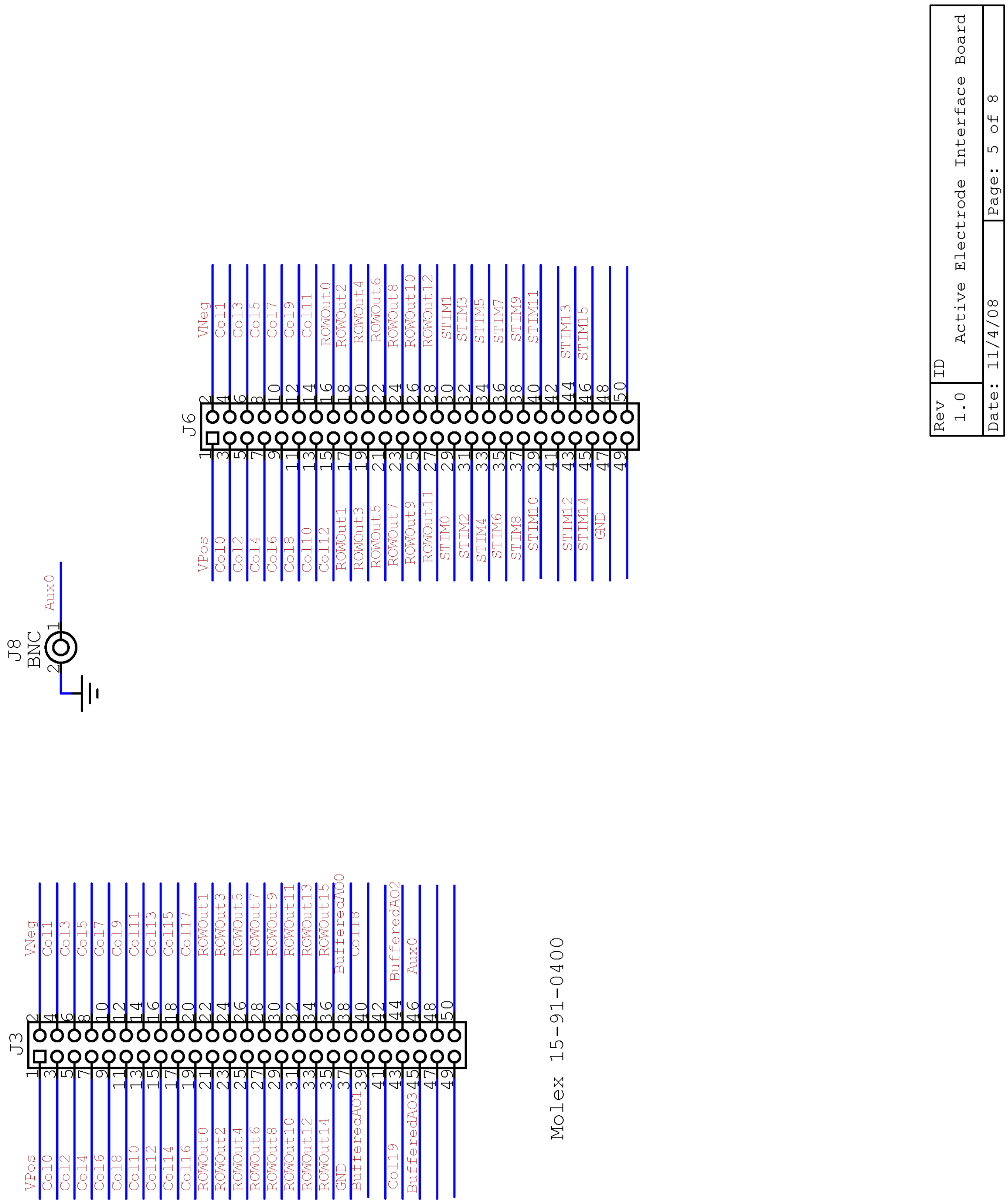

Supplementary Figure 22. Complete schematics of the custom data acquisition interface circuit board.

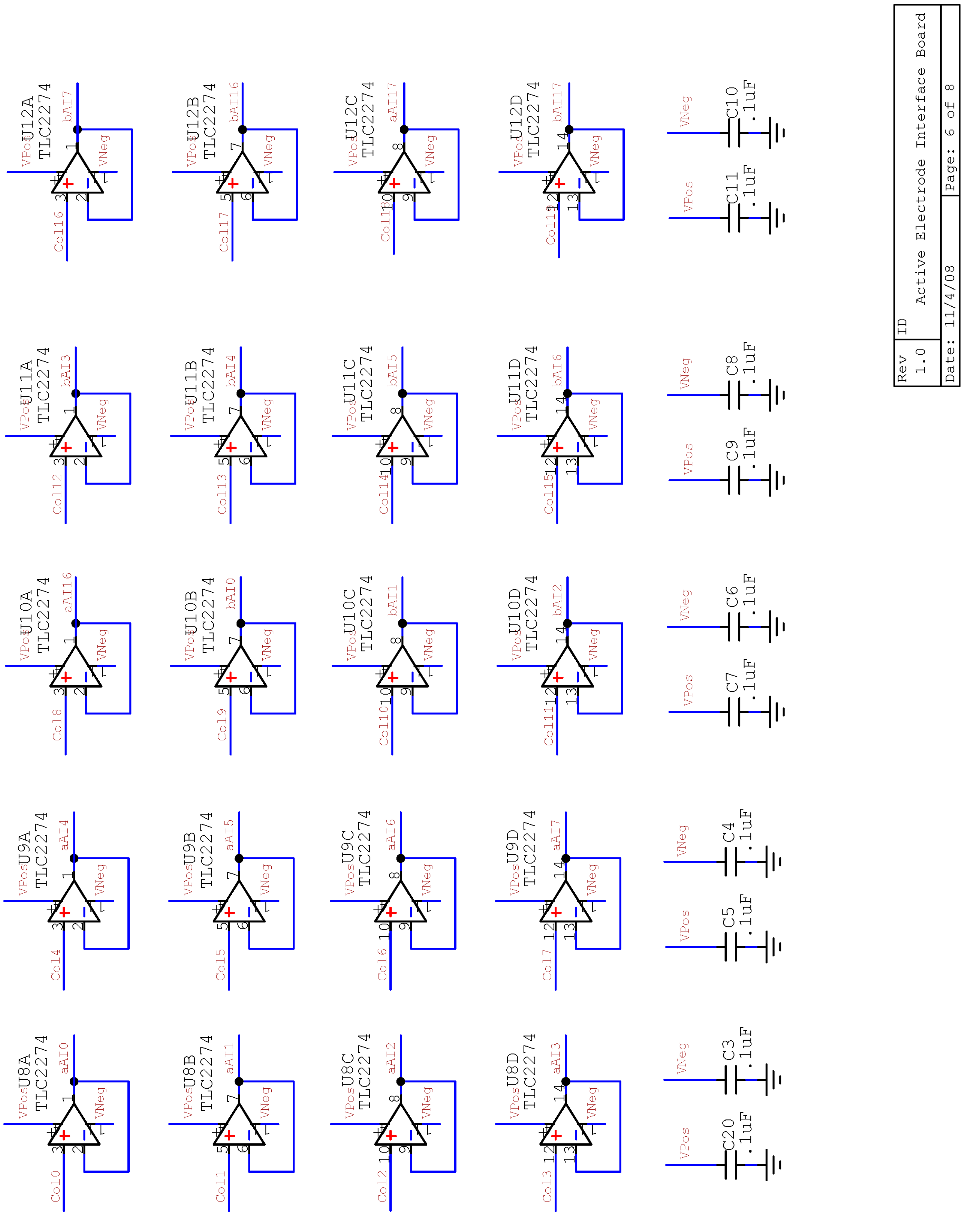

Supplementary Figure 23. Complete schematics of the custom data acquisition interface circuit board.

Nature Neuroscience: doi:10.1038/nn.2973

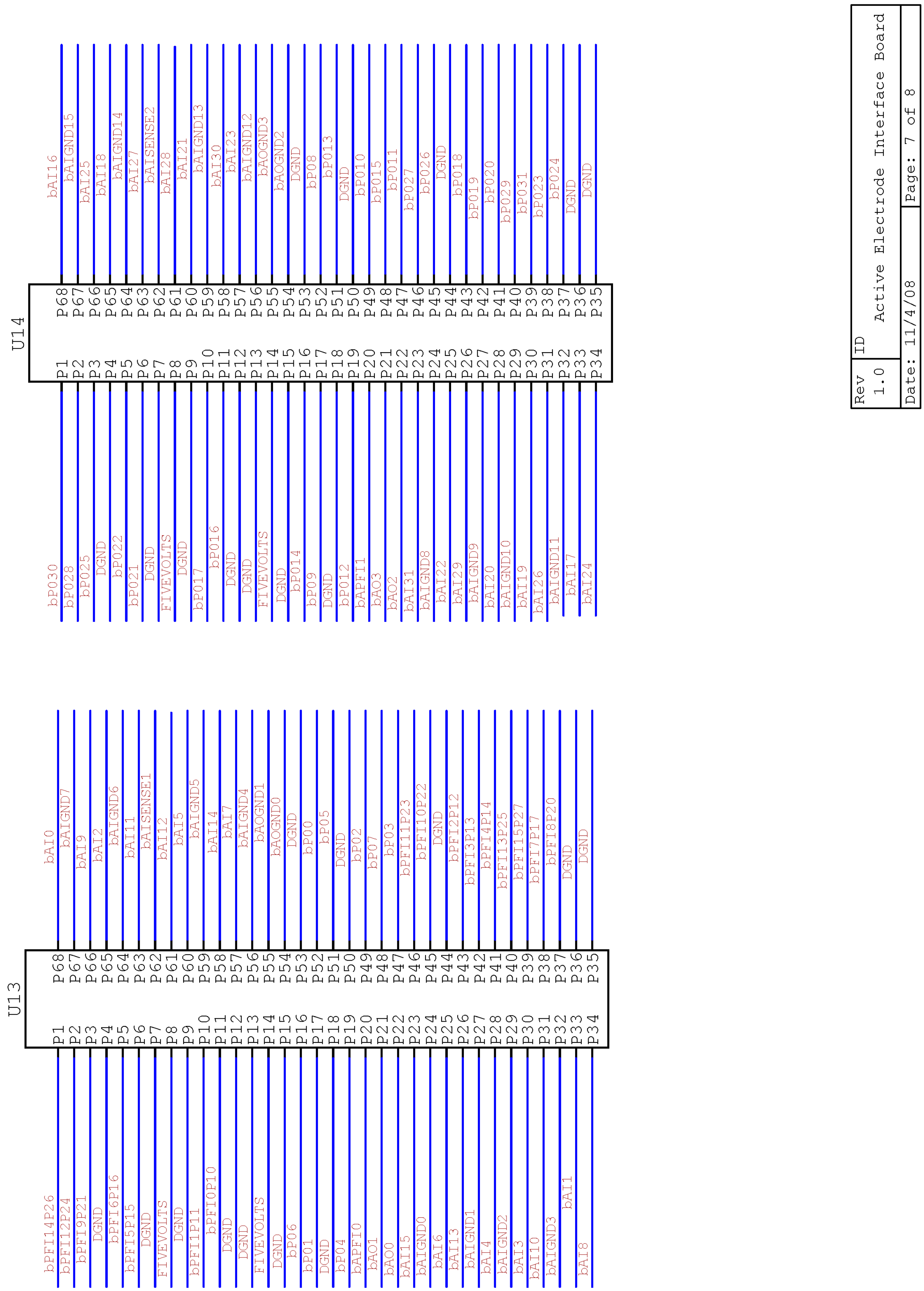

Supplementary Figure 24. Complete schematics of the custom data acquisition interface circuit board.

Nature Neuroscience: doi:10.1038/nn.2973

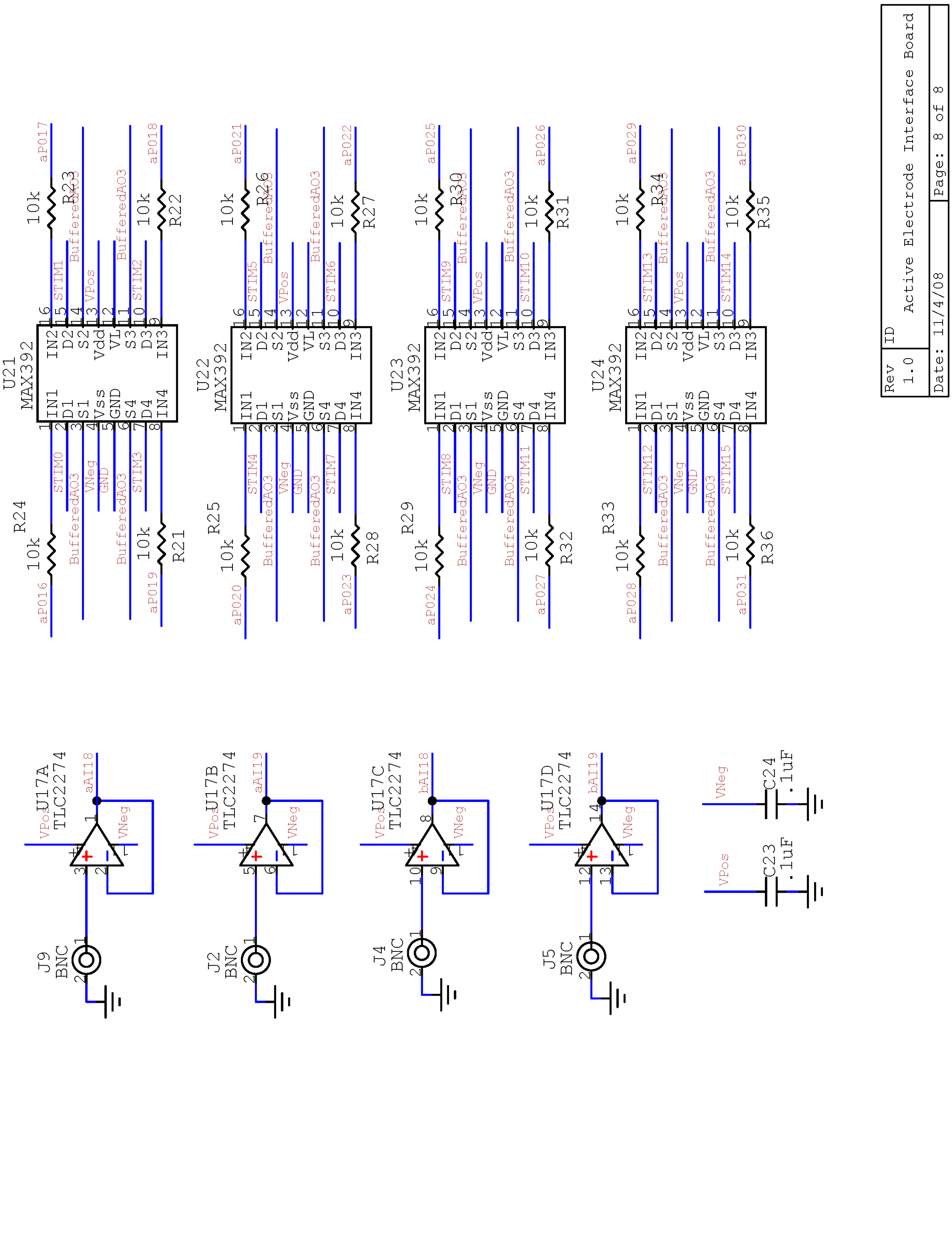

Supplementary Figure 25. Complete schematics of the custom data acquisition interface circuit board.

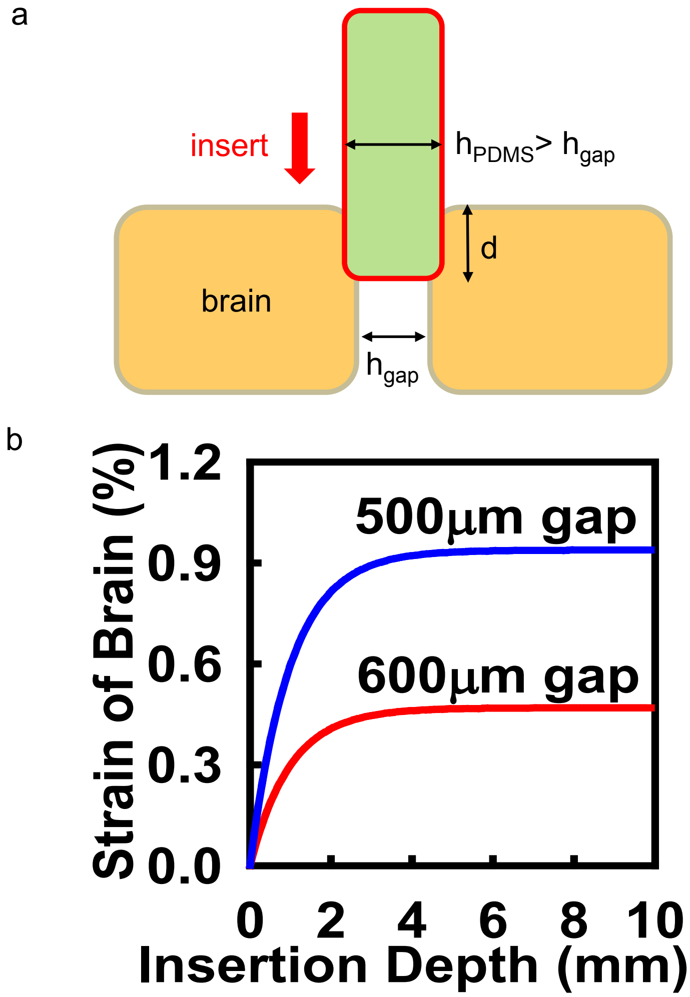

Supplementary Figure 26. Folded electrode mechanical modeling results. **a,** A diagram that shows parameter definitions for insertion model of folded electrode array. **b,** Strain induced in the brain during insertion of the folded electrode array for two different brain hemisphere spacings.

Nature Neuroscience: doi:10.1038/nn.2973

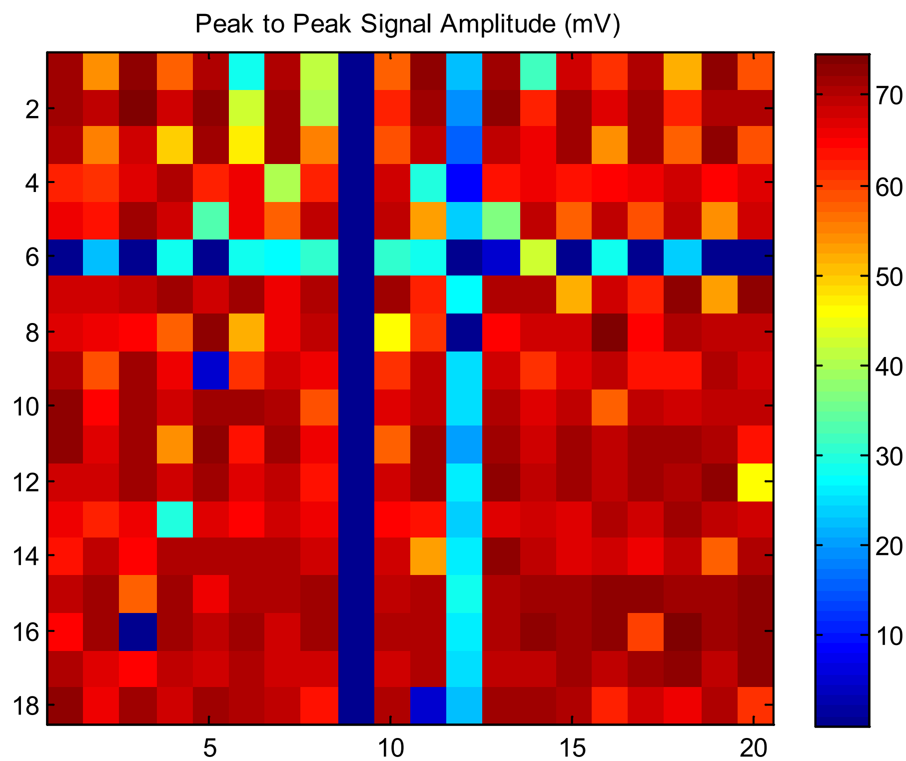

Supplementary Figure 27. Color map illustrating the spatial distribution of the electrode response to a 100mV p-p, 3.14 Hz sine wave, demonstrating the spatial uniformity of the gain of the electrode array.

Nature Neuroscience: doi:10.1038/nn.2973